Spin-dependent interfacial tunnelling and tunnel-type GMR in granular perovskite family $La_{1-x}Sr_xMnO_3$ $(0.05 \leqslant x \leqslant 0.45)$

1999 J. Phys.: Condens. Matter 11 2625

(http://iopscience.iop.org/0953-8984/11/12/017)

J. Phys.: Condens. Matter **11** (1999) 2625–2636. Printed in the UK PII: S0953-8984(99)95473-5

Spin-dependent interfacial tunnelling and tunnel-type GMR in granular perovskite family $La_{1-x}Sr_xMnO_3$ ($0.05 \leqslant x \leqslant 0.45$)

Ning Zhang†§, Fang Wang†, Wei Zhong‡ and Weiping Ding‡

† Department of Physics, Nanjing Normal University, Nanjing 210097, People's Republic of China

‡ National Laboratory of Solid State Microstructures, Nanjing University, Nanjing 210093, People's Republic of China

Received 30 June 1998, in final form 22 January 1999

Abstract. The granular perovskites $La_{1-x}Sr_xMnO_3$, with the concentration x from 0.05 to 0.5, have been fabricated by the sol–gel method. The concentration-dependent transport properties in the granular perovskites have been investigated. Spin-dependent interfacial tunnelling and the corresponding tunnel-type magnetoresistance have been observed in the samples sintered at lower temperatures in the doping range from $x = 0.05$ to 0.45 for the temperatures below the Curie point. The magnetization, the heat capacity and the oxygen stoichiometry for the sample family have been measured to show that the interfacial tunnelling stems from the magnetic difference between the surfaces and the cores of the grains, and that the tunnel-type GMR originates from the field-induced change of the surface magnetic configuration.

1. Introduction

Recently, it was reported that fine particle manganese perovskites [1, 2] showed giant magnetoresistance (GMR) of a type similar to that in granular ferromagnets. The model of spin-polarized intergranular tunnelling suggested by Hwang *et al* [3] provided a reasonable clue to discuss the magnetic and transport properties of the granular perovskites. Our preliminary study in the subject [4] furthermore demonstrated that the intergranular tunnelling resulted from a spin-dependent interfacial effect.

In [4], we have reported the grain-size-dependent transport properties in the granular perovskite $La_{0.85}Sr_{0.15}MnO_3$. In that study, a series of polycrystalline perovskites $La_{0.85}Sr_{0.15}MnO_3$ with different grain sizes was fabricated by using the sol–gel method. The average grain sizes of the granular perovskites were estimated by means of the Scherrer formula [5] through measuring the linewidths of x-ray patterns. For the samples with grain size in the range 100–200 nm, a set of regularly changing double-peaked curves of resistivity versus temperature $\rho(T)$ was obtained. Also, the giant magnetoresistance (GMR) effect similar to that observed in granular transition metals, i.e., magnetoresistance monotonically decreases with increasing temperature, and a crystal intrinsic colossal magnetoresistance (CMR) were simultaneously observed. With increasing grain size, the GMR effect gradually weakens and the intrinsic CMR effect becomes prominent. In the meantime, the ferromagnetic phase transition was found to broaden as the grain size decreased. Based on these observations, a model of spin-dependent interfacial tunnelling was suggested. In that model, the interfaces

§ Contact author.

0953-8984/99/122625+12$19.50

between neighbouring grains are assumed to be the intergranular barriers due to the magnetic disorder in the grain surfaces. An itinerant electron, which comes from the 3d shell e_g^1 orbit of the Mn^{3+} ion, can hop from grain to grain through spin-dependent interfacial tunnelling. The probability of electrons tunnelling across the intergranular barrier can be calculated by considering an *extra energy* related to double exchange interaction [6] arising when the ionic spins in the grain cores are parallel and the ionic spins in grain surfaces are not parallel, while the spin of the itinerant electron is conserved in tunnelling. Then, a resistivity formula describing the interfacial tunnelling was developed to explain the unusual transport properties of the porous granular system. The theoretical calculation was found to be in good agreement with the experimental results.

Recently, we have observed that the interfacial tunnelling and the tunnel-type magnetoresistance (TMR) can exist over a wide doping regime for the perovskite, from the so-called charge ordering spin-canted insulator (CNI) [7] to the antiferromagnetic insulator (AFM) [8], but not only in the ferromagnetic metallic perovskites, such as $La_{0.67}Ca_{0.33}MnO_3$ [1], or $La_{0.85}Sr_{0.15}MnO_3$ [4].

In this study, we will present an observation of the spin-dependent interfacial tunnelling and the TMR in the granular perovskite family $La_{1-x}Sr_xMnO_3$ ($0.05 \leqslant x \leqslant 0.45$). We will put the emphasis of the investigation on the magnetic and transport properties of the samples with $x \leqslant 0.15$ and $x \geqslant 0.35$ to show the generality of the interfacial tunnelling and the related TMR.

2. Sample characterization

The granular samples $La_{1-x}Sr_xMnO_3$ under investigation were fabricated by the sol–gel method as reported previously [4], with the nominal concentration x changed from 0.05 to 0.5. The resultant powder was pressed into strips of $20 \times 1 \times 4$ mm^3, then sintered at different temperatures in air for the same long period (6 h) to obtain polycrystalline samples with various grain sizes. X-ray diffraction measurements revealed that the fabricated samples were in the perovskite structure with no secondary phases. Most of the 1400 °C or lower temperature sintered samples are in the rhombohedral structure (with space group $R\bar{3}c$), while some of them are in orthorhombic (with space group *Pbnm*) and rhombohedral coexisting phases.

Samples sintered at two temperatures, 1000 and 1400 °C, are studied, except the sample system $La_{0.82}Sr_{0.18}MnO_3$. The average grain size estimated from scanning electron microscopy (SEM) are 0.08–0.12 μm for 1000 °C sintered samples and 1–1.5 μm for the 1400 °C sintered ones, respectively. In addition, through SEM, the samples are found to be more porous when sintered at lower temperatures. This indicates that there are fewer conductive channels in the low-T sintered samples, so the conductances of these samples are lower than that in high-T sintered ones.

The oxygen stoichiometries of the different doped samples are found to decrease a little as sintering temperature T_s increases. The oxygen content in the samples is determined by the temperature programmed reduction (TPR) technique [9], where $Ar + H_2$ (18.5% v/v) mixed gas flushes over the sample, which is heated at a linear programmed rate, and the concentration of H_2 in the mixed gas is monitored simultaneously by thermal conductivity detector (TCD). The oxygen content in the sample is deduced from the change of H_2 amount in reaction with the sample. Measured values obtained from the TPR method are believed to be reliable to within about 3%. The relative change of the oxygen content is within 2.3% when the T_s is increased from 1000 to 1400 °C. The average valence state of Mn is also measured, by the technique of inductively coupled plasma atomic emission spectroscopy (ICP), from which the quantities of

the cations in the sample can be obtained (Leeman-PS1 ICP equipment is used in the study). The results have been found to be consistent with that of oxygen content measurements. Using the values obtained from ICP or TPR, two kinds of expression for the chemical formula of the samples are possible, i.e., B-site-deficient-type $La_{1-x}Sr_xMn_\delta O_3$ and oxygen-deficient-type $La_{1-x}Sr_xMnO_z$. For brief of the discussion, we use the nominal composition $La_{1-x}Sr_xMnO_3$ for all samples in this study, except in the discussion of the oxygen content.

3. Experimental results and discussion

In order to understand the tunnelling behaviour in the various doped samples, we firstly show the $\rho(T)$ curves for different temperature sintered $La_{0.82}Sr_{0.18}MnO_3$, which is a typical ferromagnetic perovskite, in figure 1. It can be seen that: (1) a broad resistivity peak is observed well below the Curie point T_C ($\sim$285 K) for the 900 °C sintered sample; (2) a sample sintered at a temperature between 1000 and 1300 °C shows a double-peaked $\rho(T)$ curve, with a broad peak well below T_C and a sharp one near T_C. With increasing T_s, the former gradually disappears and the latter continuously grows; (3) the 1400 °C sintered sample shows only a sharp peak near T_C.

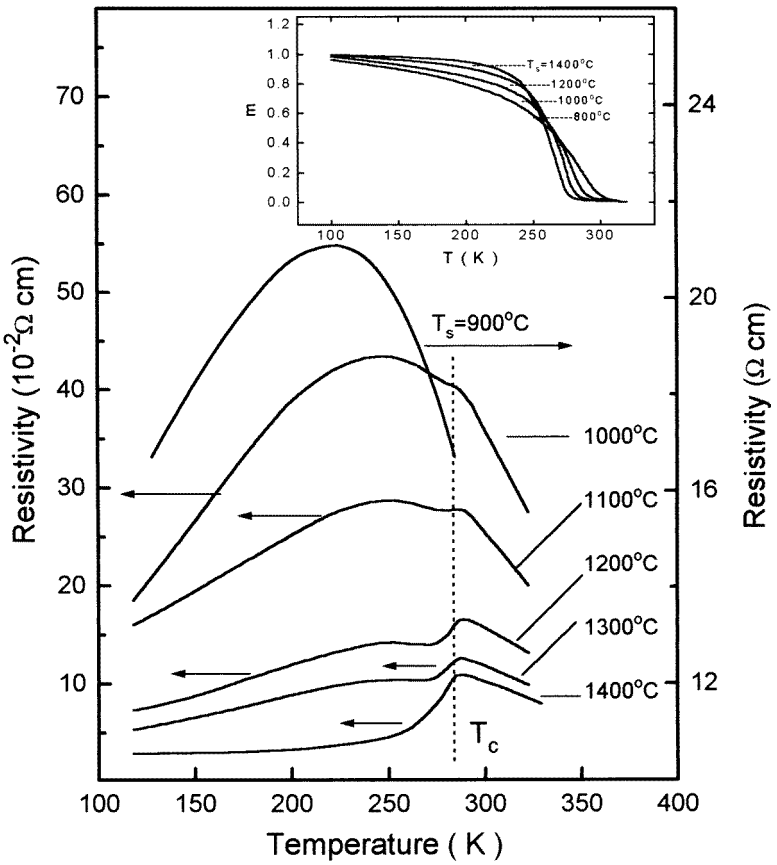

Figure 1. Resistivity against temperature for different temperature sintered $La_{0.82}Sr_{0.18}MnO_3$; inset is the magnetization against temperature for different temperature sintered $La_{0.82}Sr_{0.18}MnO_3$.

It is easy to prove that the 1400 °C sintered sample basically exhibits the crystal intrinsic transport. The sharp peak near T_C just reflects the so-called metal–insulator transition in the perovskite crystals [10]. However the broad peak is difficult to relate to an intrinsic property since it is located at a temperature much lower than T_C. This phenomenon may be particular to the granular manganese perovskite, and has never been seen in any other kinds of granular ferromagnet [11]. It has been suggested in [4] that the broad resistivity peak results from a spin-dependent interfacial tunnelling, which stems from the difference in magnetic state between the grain surface and the core. Evidence for that given there is that the ferromagnetic phase transition temperature T_C broadens with decreasing T_s or grain size, as shown in the inset of figure 1. The T_C is defined here as the temperature at the point with the maximum slope $(\mathrm{d}m/\mathrm{d}T)$ on the $m(T)$ curve. The T_C-broadening is helpful to explain the existence of the magnetic disorder in the grain surface. The transport behaviour of the 900 °C sintered sample can then be expected to represent typical interfacial tunnelling, and figure 1, in fact, exhibits a transformation from the interfacial tunnelling to the intrinsic transport of the perovskite.

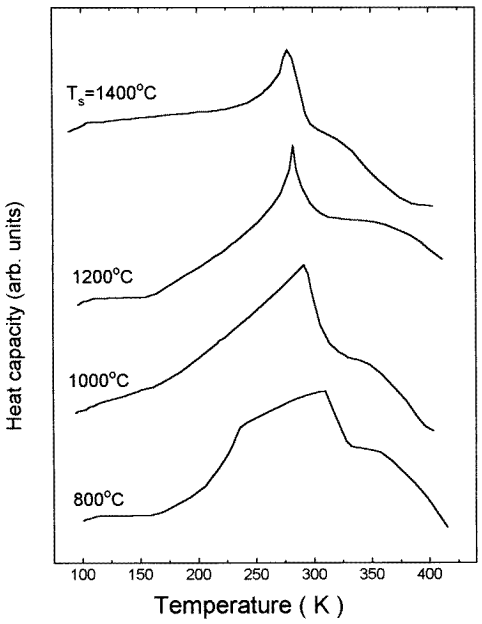

Figure 2. Heat capacity against temperature for different temperature sintered $La_{0.82}Sr_{0.18}MnO_3$.

Further evidence given here for showing the magnetic disorder in the grain surface is the alteration of the heat capacity in the sample system as the grain size decreases, as shown in figure 2. The heat capacity is obtained from differential scanning calorimetry (DSC) experiment. The temperature is changed at the rate of $(\mathrm{d}T/\mathrm{d}t)$ of 5 °C min^{-1} in the DSC measurements. The capacity can then be given as $C = (\mathrm{d}Q/\mathrm{d}t)/(\mathrm{d}T/\mathrm{d}t)$, where $(\mathrm{d}Q/\mathrm{d}t)$ is the measured heat flow. The DSC curves exhibit a peak indicating a second order phase transition, and all the phase transition temperatures are found to be consistent with the ferromagnetic transition temperatures T_C. Meanwhile, the phase transition temperature also broadens to lower temperature as the grain size decreases, and the broadening is basically compatible with the T_C-broadening. It is well known that the peak-type jump of heat capacity reflects the ferromagnetic phase transition. The jump of heat capacity at lower temperature can then be expected to reflect the ferromagnetic phase transition in grain surface. This means

that the T_C in the grain surface is lower than that in the core. It is known from the Heisenberg theory of ferromagnetism [12] that the ferromagnetic transition temperature can be expressed as $T_C = 2qJ/k$, where q is the coordination number, J the exchange integral between neighbouring atoms and k the Boltzmann constant. On the one hand, the average coordination number q in the surfaces is lower; on the other hand, the overlap between neighbouring atoms is also lower due to the coordination number being lower, and so is the exchange integral J, thus the T_C in the grain surface is certainly lower than that in the core. In other words, the grain surfaces become paramagnetic or magnetically disordered at lower temperatures than the grain cores do. Considering that the distribution of the grain sizes in the present system, especially in the lower temperature sintered samples, is inhomogeneous, the broadening of the jump of the heat capacity as grain size decreases should be expected to indicate the T_C-broadening as the surface volume fraction increases, or the grain size decreases.

However, a change of oxygen content can also induce a change in the magnetism of the perovskites [13]. To discriminate the origin of the T_C-broadening, the oxygen content versus T_s has been measured. The data for the granular system $La_{0.82}Sr_{0.18}MnO_z$ is shown in figure 3. The oxygen stoichiometry z decreases from 2.985 to 2.917 as T_s increases from 900 to 1400 °C. Such minute (<2.3%) differences in oxygen stoichiometry have been found to have some effect on T_C-shift, but barely influence T_C-broadening [13, 14]. A small (for instance, <3.0%) increase of oxygen vacancies can only decrease the carrier concentration, which can make the T_C shift [14, 15], while greater oxygen-deficiency could give rise to a serious distortion of the MnO_6 octahedra [15] besides decreasing the carrier concentration, that could induce grave alteration of the magnetic and transport properties of the compounds [15, 16]. In short, the regular T_C-broadening observed here can be more likely attributed to surface magnetic disorder. This therefore causes a magnetic difference between core and surface, then an intergranular barrier, and also the TMR [4].

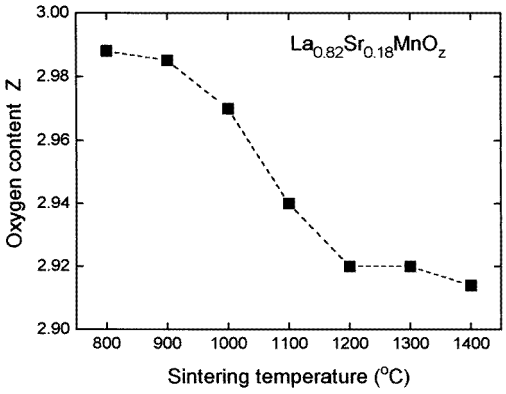

Figure 3. Oxygen content against sintering temperature for $La_{0.82}Sr_{0.18}MnO_z$.

More convincing evidence for the transformation is the magnetoresistive behaviour of the granular system $La_{0.82}Sr_{0.18}MnO_3$, as shown in figure 4. It can be seen that, as T_s increases from 900 to 1400 °C, the magnetoresistance versus temperature MR(T) systematically changes from a type similar to that observed in most granular ferromagnets [11], as shown in the inset of the figure, to the perovskite intrinsic form, i.e., the CMR [10]. The magnetoresistance ratio is defined here as $MR = [R(0) - R(H)]/R(0)$ where $R(0)$ and $R(H)$ are the resistivity at zero field and under an external field, respectively. The inset shows the MR(T) curves for a typical granular transition metal, Cu–Co alloys [11]. Since the GMR effect in granular ferromagnets

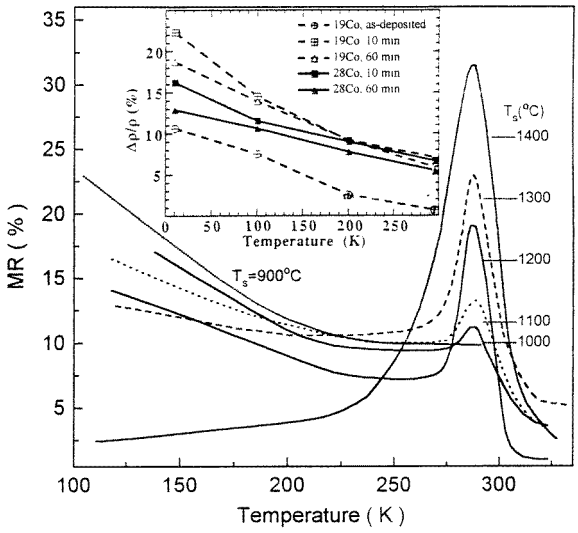

Figure 4. Magnetoresistance against temperature under an external field $H = 1.5$ T for different temperature sintered $La_{0.82}Sr_{0.18}MnO_3$, MR $= [R(0) - R(h)]/R(0)$; inset shows the MR(T) curve for granular ferromagnets Cu–Co from Berkowitz *et al*.

is generally believed to originate from an intergranular tunnelling, it is reasonable to attribute the magnetoresistance of the 900 °C sintered sample to a tunnelling behaviour. This has also been demonstrated by the surface magnetic disorder [4].

Next, we show that the spin-dependent interfacial tunnelling and the related TMR effect can exist in the granular perovskites $La_{1-x}Sr_xMnO_3$ with the concentration x over a considerably wide region, from $x = 0.05$ to 0.45, which well exceeds the range of the existence of the intrinsic CMR.

Figure 5 shows the transport properties at zero field and under an applied field $H = 1.5$ T and the corresponding magnetoresistances for the 1400 °C sintered and differently Sr-doped $LaMnO_3$. It is the same as earlier seen in the granular system $La_{0.82}Sr_{0.18}MnO_3$, the 1400 °C sintered samples mainly exhibit the intrinsic behaviour of magnetic transport, which is identical with that detected from the crystals of the hole doped manganese perovskite, and the CMR effect. No interfacial tunnelling and the TMR are observed in these perovskites. The doping regime in which the CMR can be found is about $x = 0.1$ to 0.4. In fact, for $x = 0.1$ and 0.4, the CMR effect is already very small, ∼5% under an applied field $H = 1.5$ T.

The same measurements as performed in figure 5 for the 1000 °C sintered and differently doped samples are shown in figure 6. Most of the samples are also found to show a double-peaked curve of resistivity $\rho(T)$, with a sharper peak near T_C, and a broader one well below T_C, the same as earlier seen in the granular system $La_{0.82}Sr_{0.18}MnO_3$. So we are able to believe that the former reflects the crystal intrinsic transport property of the perovskite, and the latter result from the interfacial tunnelling. In addition, figure 6 shows that, although the $\rho(T)$ curve undergoes various changes with the change of doping level, all the 1000 °C sintered samples exhibit a granular ferromagnet-like curve of MR(T), i.e., a monotonically decreasing MR(T) curve, except for a small peak near T_C, which is just the intrinsic CMR peak for the manganese perovskites.

Furthermore, the phenomenon of T_C-broadening has also been observed universally to exist in the differently doped and 1000 °C sintered perovskites, as shown in figure 7, where

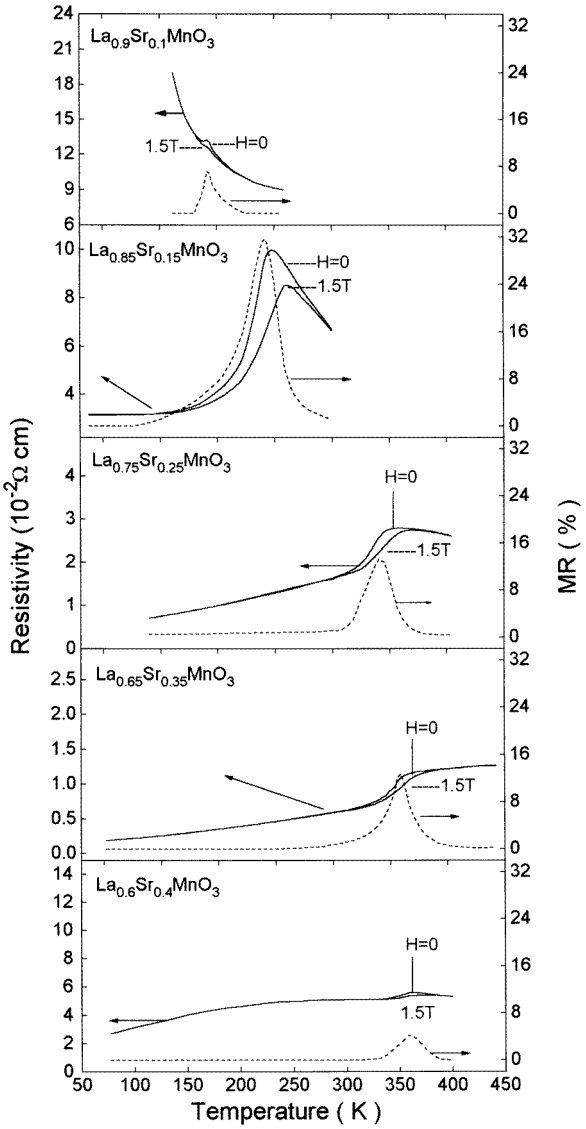

Figure 5. Resistivity against temperature at zero field and under an external field $H = 1.5$ T (solid lines) and the corresponding MR(T) curves (dotted lines) for 1400 °C sintered and different Sr-doped $LaMnO_3$.

m is the magnetization normalized to the saturated value. This point suggests that the surface magnetic disorder can exist in all the different doped samples. In addition, similar to what is observed in the granular system $La_{0.82}Sr_{0.18}MnO_3$, no greater than 2.3% relative change of oxygen content has been detected from the samples with the same nominal concentration but sintered at 1000 and 1400 °C, respectively. The data showing the oxygen stoichiometry for the differently doped samples are shown in table 1, where Z and Z' are the oxygen stoichiometries for 1400 and 1000 °C sintered samples respectively. According to the data in table 1, we also believe that the change of oxygen stoichiometry due to the difference of sintering temperatures

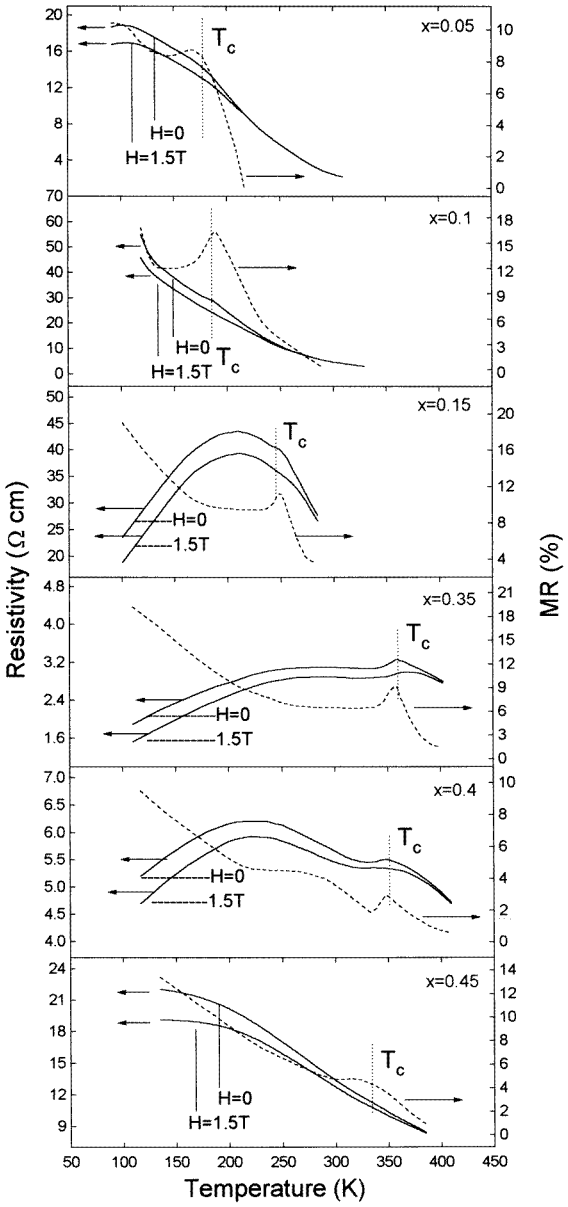

Figure 6. Resistivity against temperature at zero field and under an external field $H = 1.5$ T (solid lines) and the corresponding MR(T) curves (dotted lines) for 1000 °C sintered and different Sr-doped $LaMnO_3$.

for the variously doped granular perovskites is not the main cause of the T_C-broadening, whereas magnetic disorder in the surface can be expected to result in it.

All the results displayed in figures 6 and 7 suggest that the behaviour of interfacial tunnelling and the TMR related to double exchange interaction can universally exist in the granular manganese perovskite. Comparing the $m(T)$ curves of 1000 °C sintered samples with those of 1400 °C sintered ones, and combining figure 6 with figure 7, there are several

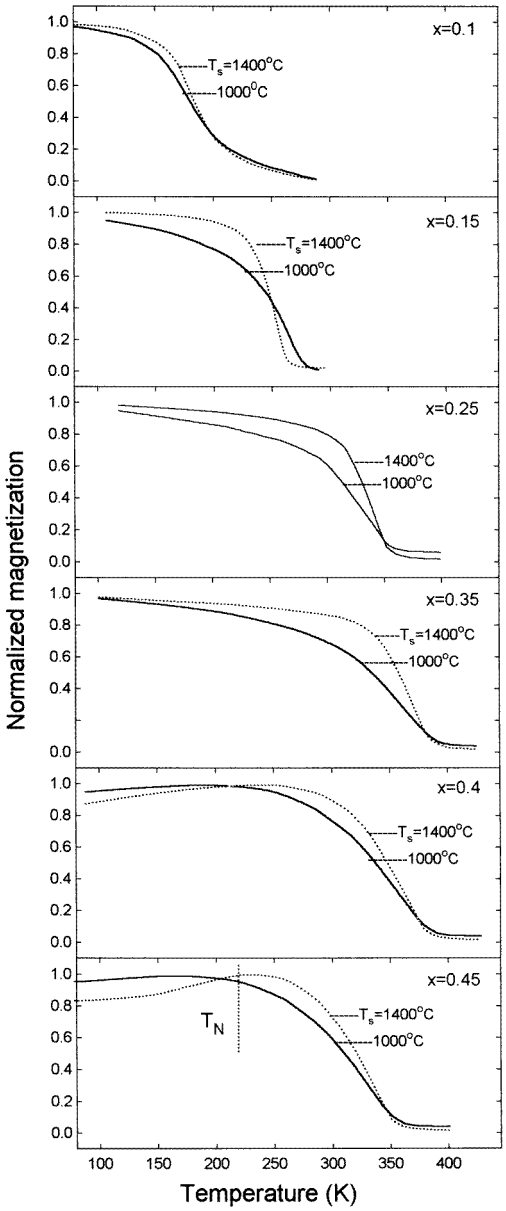

Figure 7. Normalized magnetization against temperature for 1000 °C (solid lines) and 1400 °C sintered (dotted lines) and different Sr-doped $LaMnO_3$. T_N is the Néel temperature.

noticeable points as follows: (1) Since the TMR can exist at all the temperatures below T_C, the higher the T_C, the wider temperature range where the TMR emerges. (2) For some granular samples, not only the TMR but also the resistivity can be invariant in a considerably wide region of temperature, such as the 1000 °C sintered sample with $x = 0.35$. This property must result from the coexistences of the interfacial tunnelling and the intrinsic transport, and the TMR and CMR. (3) For the granular samples with their magnetic order in a spin-canted state

Table 1. Values of oxygen content for 1000 and 1400 °C sintered and different Sr-doped $LaMnO_3$.

	$x = 0.05$	$x = 0.15$	$x = 0.35$	$x = 0.45$
Z'	2.978	2.980	2.980	2.982
Z	2.910	2.915	2.925	2.914
$\frac{Z'-Z}{Z'}$	2.28%	2.18%	1.85%	2.28%

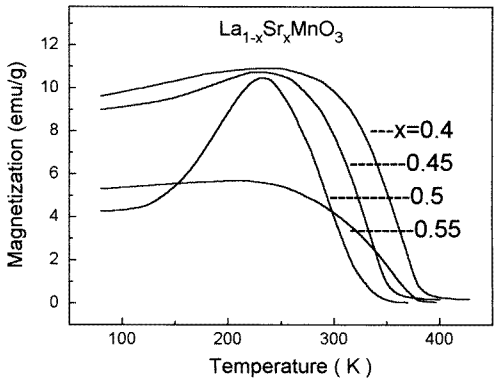

Figure 8. Magnetization versus temperature under an external field $H = 0.5$ T for 1400 °C sintered and different Sr-doped, from $x = 0.4$ to 0.55, $LaMnO_3$.

[7], for instance the sample with $x = 0.05$, the intrinsic CMR can scarcely be detected (<3% under an applied field $H = 1.5$ T, which is obtained from bulk crystal) in it; however the TMR can also be observed. This suggests again that the TMR does not relate to the magnetism in grain cores but only depends on the relative magnetization of the core to the surface. By the way, the long tails of the $m(T)$ curves for $x = 0.05$ and 0.1 is not surprising. It can often be observed in the crystals with lower doping levels [17, 18], which may be a result of an incompletely released structure–magnetism coupling [18], which is usually related to the preparing conditions of samples [17]. (4) It is of special interest to observe that the TMR can emerge in some granular samples with mixed magnetic orders.

The 1400 °C sintered $La_{0.55}Sr_{0.45}MnO_3$ shows partial antiferromagnetic order below about 220 K (the Néel point), and ferromagnetic order between 220 and 345 K (the Curie point). In practice, the phenomenon of partial antiferromagnetism initially emerges for $x = 0.4$. It becomes prominent with increasing x, and is most conspicuous at $x = 0.5$, as shown in figure 8, which presents the magnetization versus temperature for the samples doped from $x = 0.4$ to 0.55 and sintered at 1400 °C. The behaviour of magnetization shown in figure 8 is basically consistent with the report in the literature [8]. From figure 8, it is worthwhile to point out that the phase diagrams provided in [7] may be incomplete. Since the 1400 °C sintered samples present the intrinsic properties, we then can expect that the grain cores of the 1000 °C sintered samples have the same magnetic order as that in 1400 °C sintered ones. In other words, the grain cores of the 1000 °C sintered $La_{0.55}Sr_{0.45}MnO_3$ should have partial antiferromagnetic order. However, its surfaces could be in a ferromagnetic or paramagnetic state. This may explain why the 1000 °C sintered $La_{0.55}Sr_{0.45}MnO_3$ shows no evident antiferromagnetism. This means that a strong influence of surface magnetism exists in the sample. This magnetic difference can also make the interface a potential barrier below 220 K, perhaps a potential wall because the cores have greater resistance in that case due to being in the antiferromagnetic

state. In fact, from [4], the tunnel resistivity in the granular perovskite can be approximately expressed as

$$\rho_t \propto \frac{1}{D} \exp\left\{ b \left[\frac{(Dm - 3wm_s)^2}{(D-3w)^2} - m_s^2 \right]^{1/2} \right\}$$

where b is a constant related to the transfer integral between neighbouring Mn ions, m and m_s are the normalized magnetization respectively in the granular system and the grain surfaces, D is the average grain size, and w is the mean thickness of grain surfaces.

From the equation above, the tunnel resistivity depends not on the total magnetization of the granular system, but on the grain size and the difference between m and m_s. So long as the magnetic difference exists, the interfacial tunnelling can be observed no matter what magnetic order is in the core. The TMR can then be expected to take place not only in the samples with their concentration in the regime of a ferromagnetic metal but also in part of the regime of a ferromagnetic insulator, even in some samples with antiferromagnetic order, such as the 1000 °C sintered $La_{0.55}Sr_{0.45}MnO_3$. On the other hand, since the tunnel resistivity is inversely related to the grain size (see the equation above), the smaller the grain size, the more sensitive the tunnel resistance is to the change of the difference in magnetic state, and the larger TMR may be.

In summary, the magnetoresistive behaviours observed in this study furthermore demonstrate that: (1) the interfacial tunnelling must be a universal phenomenon that exists in granular manganese perovskites; (2) the transport properties of the granular perovskites depend on the magnetism of the grain surface but not on the magnetic moments of neighbouring grains. This point discriminates a granular perovskite from other granular ferromagnets in transport mechanisms, and makes a granular perovskite particular in transport behaviour on the one hand, but similar to other granular ferromagnets in magnetoresistive properties on the other hand.

Acknowledgment

This work was supported by the National Natural Science Foundation of China (grant No 19874031).

References

[1] Sànchez R D, Rivas J, Vàzquez-Vàzquez C *et al* 1996 *Appl. Phys. Lett.* **68** 134
[2] Mahesh R, Mahendiran R, Raychaudhuri A K and Rao C N R 1996 *Appl. Phys. Lett.* **68** 2291
[3] Hwang H Y, Cheong S-W, Ong N P and Batlogg B 1996 *Phys. Rev. Lett.* **77** 2041
[4] Zhang Ning, Ding Weiping, Zhong Wei, Xing Dingyu and Du Youwei 1997 *Phys. Rev.* **56** 8138
[5] Mendelson M I 1969 *J. Am. Ceram. Soc.* **52** 443
[6] Zener C 1951 *Phys. Rev.* **82** 403
Anderson P W and Hasegawa H 1955 *Phys. Rev.* **100** 675
deGennes P G 1960 *Phys. Rev.* **118** 141
[7] Urushibara A, Moritomo Y and Arima T *et al* 1995 *Phys. Rev.* B **51** 14 103
Rao C N R and Cheetham A K 1996 *Science* **272** 369
[8] Schiffer P, Ramirez A P, Bao W and Cheong S-W 1995 *Phys. Rev. Lett.* **75** 3336
[9] Hurst N W, Gentry S J, Jones A and McNicol B D 1982 *Catal. Rev.* **24** 233
[10] Jin S *et al* 1994 *Sci.* **264** 413
von Helmolt R *et al* 1993 *Phys. Rev. Lett.* **71** 2331
Chahara Ken-ichi *et al* 1993 *Appl. Phys. Lett.* **63** 1990
[11] Berkowitz A E *et al* 1992 *Phys. Rev. Lett.* **68** 3745
Xiao J Q *et al* 1992 *Phys. Rev. Lett.* **68** 3749
[12] Heisenberg W 1928 *Z. Phys.* **49** 619

[13] De Léon-Guevara A M, Berthet P and Berthon J *et al* 1997 *Phys. Rev.* B **56** 6031
[14] Ju H L, Gopalakrishnan J, Peng J L, Li Qi, Xiong G C, Venkatesan T and Greene R L 1994 *Phys. Rev.* B **51** 6143
Jirak Z *et al* 1985 *J. Magn. Magn. Mater.* **53** 153
[15] Radaelli P G, Iannone G, Marezio M, Hwang H Y, Cheong S-W, Jorgensen J D and Argyriou D N 1996 *Phys. Rev.* B **56** 8265
[16] Booth C H, Bridges F, Kwei G H, Lawrence J M, Cornelius A L and Neumeier J J 1998 *Phys. Rev. Lett.* **80** 853
[17] Itoh M, Nishi K, Yu J-D and Inaguma Y 1997 *Phys. Rev.* B **55** 14 408
[18] Argyriou D N, Mitchell J F and Potter C D *et al* 1996 *Phys. Rev. Lett.* **76** 3826